AD-A180 185 COMPUTATIONAL METHODS FOR LOW VELOCITY PERFORATION OF METALLIC PLATES(U) MATERIALS RESEARCH LABS ASCOT VALE (AUSTRALIA) R WOODWARD DEC 86 MRL-R-1036 1/1

UNCLASSIFIED F/G 11/6.1 NL

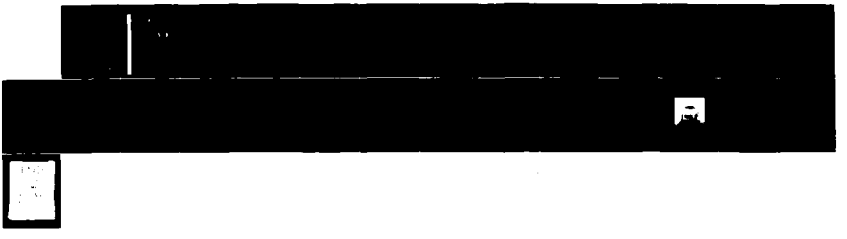

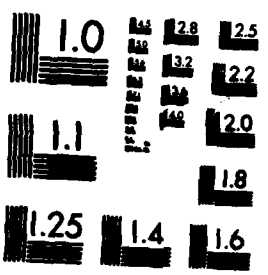

AR-005-109

(12)

DEPARTMENT OF DEFENCE

DEFENCE SCIENCE AND TECHNOLOGY ORGANISATION

MATERIALS RESEARCH LABORATORIES

MELBOURNE, VICTORIA

REPORT

MRL-R-1036

COMPUTATIONAL METHODS FOR LOW VELOCITY PERFORATION OF METALLIC PLATES

R. Woodward

Approved for Public Release

DEPARTMENT OF DEFENCE
MATERIALS RESEARCH LABORATORIES

REPORT

MRL-R-1036

COMPUTATIONAL METHODS FOR LOW VELOCITY PERFORATION OF METALLIC PLATES

R. Woodward

ABSTRACT

Low velocity perforation problems, whether they be from a large scale missile impact or a very small fragment, are characterized by the introduction of both intense localized deformations and low strain structural deformations of the target. This report describes techniques which can be used to obtain estimates of the response of a thin plate to such an impact. Simple analytical approaches which are amenable to hand calculation, and also a structural model which is computationally very efficient are described. The solutions of these techniques are compared with empirical data for a range of problems in order to present clearly the scope of applicability and the accuracy of the methods.

Approved for Public Release

POSTAL ADDRESS: Director, Materials Research Laboratories
P.O. Box 50, Ascot Vale, Victoria 3032, Australia

SECURITY CLASSIFICATION OF THIS PAGE **UNCLASSIFIED**

DOCUMENT CONTROL DATA SHEET

REPORT NO.	AR NO.	REPORT SECURITY CLASSIFICATION
MRL-R-1036	AR-005-109	Unclassified

TITLE

Computational methods for low velocity perforation of metallic plates

AUTHOR(S)

R. Woodward

CORPORATE AUTHOR

Materials Research Laboratories
PO Box 50,
Ascot Vale, Victoria 3032

REPORT DATE	TASK NO.	SPONSOR
December, 1986	ARM 84/153	ARMY

FILE NO.	REFERENCES	PAGES
G6/4/8-3316	28	23

CLASSIFICATION/LIMITATION REVIEW DATE

CLASSIFICATION/RELEASE AUTHORITY

Superintendent, MRL
Metallurgy Division

SECONDARY DISTRIBUTION

Approved for Public Release

ANNOUNCEMENT

Announcement of this report is unlimited.

KEYWORDS

Penetration, Deformation, Models, Perforation, Computation

COSATI GROUPS 20110 19040

ABSTRACT

Low velocity perforation problems, whether they be from a large scale missile impact or a very small fragment, are characterized by the introduction of both intense localized deformations and low strain structural deformations of the target. This report describes techniques which can be used to obtain estimates of the response of a thin plate to such an impact. Simple analytical approaches which are amenable to hand calculation, and also a structural model which is computationally very efficient are described. The solutions of these techniques are compared with empirical data for a range of problems in order to present clearly the scope of applicability and the accuracy of the methods.

CONTENTS

COMPUTATIONAL METHODS FOR LOW VELOCITY PERFORATION OF METALLIC PLATES

1. INTRODUCTION

The ability of a projectile to perforate a target can be assessed by comparing its kinetic energy with the mechanical work required to produce a hole of the appropriate size and shape in the target. Estimation of the mechanical work to produce a hole requires a knowledge of the deformation mechanisms and depends in a complex way on such aspects as shape, size, velocity and mass of the penetrator, and the impact obliquity, as well as the density, mechanical and thermodynamic properties of the target material. Two basic approaches have been adopted towards the solution to this type of problem, viz. analytical models and computer code techniques.

Analytical models of penetration are developed by limiting the scope of the problem to narrow geometric conditions. An early example was the work of Taylor [1] on the perforation of metallic plates by pointed projectiles, followed notably by Thomson [2] who produced a solution for dishing failure of thin plates. A number of models of other failure modes have been produced [3-5], which all have simple analytical solutions with an equation relating projectile critical velocity to target dimensions and material properties. In an effort to better describe the sequence of events during penetration more complex analytical approaches have developed out of the simpler solutions, in particular looking at plugging failures which are produced by flat ended projectiles [6,7]. A number of classifications of target failure have been produced and these are presented, with discussion of concepts and models in a number of reviews [8-10]. The analytical approach suffers from a loss of generality, however it has several advantages in allowing efficient parametric studies, demonstrating the physics clearly and highlighting important aspects, and the techniques generally allow some solution to a problem within reasonable time and cost constraints. Some analytical solutions are predictive because assumptions on hole size and deformation mode built into the model allow a result to be obtained with limited impact configuration and material property data. Other approaches are descriptive as they allow the progress of perforation to be analyzed but only after some post perforation measurements on hole geometry have been made.

The second approach is to use computer code techniques, finite element or finite difference, which divide both the target and the penetrator into a large number of interconnecting elements and in each element the equations of motion are solved, along with the equations of compatibility and material constitutive relations, as the problem steps forward in time. A large number of codes are available for both localized impact response and structural response, and there have been several reviews of the technology [10, 11-13]. The computer codes find their niche in combination with experiments in the detailed design of structures, and as an aid to understanding the evolution of deformation features in impact events. By themselves codes do not guarantee a complete numerical solution to a specific impact event.

There has been a keen interest in recent times in one particular class of problem which is characterized by low velocity impacts (below normal ordnance velocities) of the order of a few hundred metres per second or less, involving blunt or flat ended projectiles and relatively thin targets in comparison to the projectile diameter. Such a situation generally results in the formation and ejection of a plug from the target and a structural response evidenced by a large permanent dishing displacement of the plate. The problem is one of interest for safety in many civil and military applications. In practice it is common for the conditions to be ill-defined in that only broad estimates of likely impact situations are possible, thus the methods for solution must be adaptable and efficient. A number of recent papers [14-22] present experimental data and model solutions for cases involving plugging of plates and both empirical approaches [23] and problems of scaling [24] are considered.

In this report two methods of approaching low velocity perforation problems are presented. The first involves assessment using a simple set of analytic equations. The second approach uses a structural model which describes the sequence of dishing, stretching and plugging of the target and requires a computer solution. Comparison with empirical data and an examination of the deformations occurring in impact events enables a constructive approach to considerations of how to handle such problems. It is a prime objective of this work to provide a set of simple tools which can easily be applied, as many of the techniques presented in the literature are in outline only and require a computer program to be written by the user, or they require some experimentation which is not always possible or desirable.

2. SIMPLE MODEL SOLUTIONS

If the discussion is limited to ductile metallic targets and projectiles which are substantially non-deforming during the interaction, then it is possible to derive simple equations for perforation depending on the deformation mode. For a pointed projectile material is generally pushed radially to the side when the projectile impacts the target as in Fig. 1(a). This mode of failure is generally called ductile hole formation. Taylor [1] developed an equation for the work done in expanding a hole from zero diameter, out to the projectile diameter and this has been shown [3] to give a reasonable estimate of the work done in penetrating a target by the

ductile hole formation mode. The work done (W) is given in terms of projectile diameter (D), target thickness (h) and target strength (σ_o) by

$$W = \frac{\pi}{2} D^2 h \sigma_o \qquad (1)$$

If the target is thin (thickness less than the projectile diameter) then there is a tendency for it to bend forward in the direction of penetration and produce a dishing failure, Fig. 1(b). In this case work is done in stretching elements of target out to the diameter of the projectile and also in bending the plate. An equation for the work done is

$$W = \frac{\pi}{8} Dh\,(D + \pi h)\sigma_o \qquad (2)$$

For a flat ended penetrator, target material is constrained to move ahead of the penetrator so that a plug is pushed out, Fig. 1(c). Under these circumstances the acceleration of material ahead of the projectile must be considered as well as the plug shearing stresses, and generally significant thinning of the plug is observed. This process has been modelled in detail [6,7,16-19]; however for thick plates most of the work done is involved with shearing of the plug. Thus an underestimate can be made as the work done in simply shearing a plug of diameter D from the plate of thickness h, namely

$$W = \frac{\pi}{2\sqrt{3}} Dh^2 \sigma_o \qquad (3)$$

For thin plates impacted by flat ended projectiles dishing of the plate will also occur and this is not accounted for in equation (3).

The choice of strength or flow stress parameter (σ_o) to be used in equations (1) to (3) is determined by the fact that the processes are ones of large strain deformation and dynamic loading so that a high estimate of strength of the material is generally better. As most stress/strain data is determined at comparatively low strain rates the preferred choices have been

(a) to fit stress/strain data to a curve of the form

$$\sigma = \sigma_o \epsilon^n \qquad (4)$$

where σ and ϵ are stress and strain respectively, and the constants σ_o and n are obtained using a log/log plot. The constant σ_o which is the stress at a strain of 1.0 is used for the strength.

(b) to use the ultimate tensile strength (UTS) of the material if this is all that is available.

Using the above methodology it is generally found that equation (1) overestimates the work done in penetration, equation (3) vastly underestimates it for thin targets where dishing is a major consideration, and equation (2) is in the correct range. Examples of such results are presented later for

comparison with solutions using the structural model below. Equations (1) to (3) have the advantage that being simple, the solution can be obtained rapidly by hand.

3. STRUCTURAL MODEL

Because the problem of blunt projectile impact on a thin plate involves localized damage as well as structural deformation, a model was developed which takes both aspects into account, and is based on a rigid plastic solution for the central impact on an infinite beam developed by Symonds [25]. The basic geometry is shown in Fig. 2. Impact of a projectile of mass G at a sufficiently high velocity V_o onto an infinite beam causes shear sliding deformation at the impact site if the shear stress Q_p in the beam equals the shear yield stress of the beam material. The beam bends around a plastic hinge a distance z from the impact site. Solution of the equations of conservation of linear and angular momentum allows the position of the hinge and the velocity of rotation to be obtained as a function of time. This geometric configuration can be transformed to that of a plate if appropriate alterations are made for the moment of inertia and mass distributions. Figure 3 shows the geometry where a projectile of velocity V_o, diameter $2R_o$, and mass G impacts a plate of thickness h_o. The equations, which have been derived elsewhere [26], are outlined below with the method of solution.

Figure 3 divides the process into two stages. In stage I the plug and projectile slide at a velocity V', greater than the velocity of adjacent plate movement, V. The plate rotates about a hinge at position z. Equating the impulse of the force, Q_p, to the change in momentum on either side of the plug/plate interface gives

$$GV_o - GV' - \frac{m_o R_o^2}{2} V' = \int 2Q_p dt \qquad (5a)$$

$$= \frac{m_o z}{2} \left(R_o + \frac{1}{3} z\right) V \qquad (5b)$$

where $m_o = 2\pi\rho h_o$ (6)

- G is projectile mass,
- V_o is projectile impact velocity,
- V' is the plug velocity (projectile and plug assumed to move together)
- V is the velocity of the plate adjacent to the plug,
- h_o is the plate initial thickness,
- R_o is the projectile radius,
- z is the hinge position, measured from the plug/target interface,
- ρ is the plate density, and
- t is time.

Similarly equating the change in angular momentum to the impulse of the torque gives

$$- GV_o z + GV'z + \frac{1}{2} m_o R_o^2 V'z + \frac{1}{3} m_o z^2 V (R_o + \frac{1}{4} z) = -2\int (M_{po} + M_{pz})dt \qquad (7)$$

where M_{po} and M_{pz} are the plastic moments at the projectile radius and the hinge position respectively.

The equations differ from those of Symonds [25] in including the mass of the plug, in using a mass distribution appropriate to a plate and allowing the impact to operate over the full projectile diameter rather than at a central point.

The shear force at the plug/target interface is given by

$$Q_p = \frac{\pi}{\sqrt{3}} R_o h Y \qquad (8)$$

and the moments at the plug/target interface and at the hinge position z are given respectively by

$$M_{po} = \frac{\pi}{4} R_o h^2 Y \qquad (9a)$$

$$M_{pz} = \frac{\pi}{4} (R_o + z) h_o^2 Y \qquad (9b)$$

where Y is the material yield stress and

h is the reduced section contact area at the plug/target interface due to shearing.

Equations (5) to (9) can be combined to give a quadratic equation for z which can be solved at each time step. The initial position of the hinge z is found to be $R_o/3$ and this increases with time. Solution of the equations shows that the velocity of the plate, V, increases with time until it either shears out as a plug or it equals the plug/projectile velocity V'. At this point shearing of the plug ceases as the relative plug/plate velocity is zero and the plate continues to stretch as a membrane with bending continuing to occur at the hinge position z. This is referred to as stage II and the conditions are shown in Fig. 3.

To simplify the calculations in stage II it was assumed that at the projectile radius the yield stress in tension is exceeded across the full section of the plate. The membrane force F_p is then

$$F_p = \pi R_o h Y \qquad (10)$$

and the bending moment at $z = 0$ is zero. At the hinge position, z, the full plastic moment, M_{pz} is again given by equation (9b). However, because of the membrane force F_p a reduced moment M'_{pz} acts [27,28], which is given in terms of M_{pz} as

$$M'_{pz} = M_{pz} \left(1 - \left[\frac{R_o h}{(R_o + z)h_o}\right]^2\right) \tag{11}$$

The equations for angular and linear momentum, respectively, in stage II are

$$\frac{1}{2} GZ\Delta V \cos\theta + \frac{1}{4} m_o R_o^2 z\Delta V \cos\theta + \frac{1}{6} m_o z^2 \left(R_o + \frac{1}{4} z\right) \Delta V \cos\theta$$

$$= -(M'_p + F_p z \sin\theta)\,\Delta t \tag{12}$$

$$G\Delta V + \frac{1}{2} m_o R_o^2 \Delta V + \frac{1}{2} m_o z \left(R_o + \frac{1}{3} z\right) \Delta V + m_o \left(R_o + \frac{2}{3} z\right) V\Delta z = 0 \tag{13}$$

where θ is the angle through which the plate is bent,

Δt is the time step,

ΔV is the change in velocity and

Δz the change in hinge position.

Terms of the type $\Delta z \Delta V$ have been ignored. As z is known at the start of stage II, equation (12) can be solved for ΔV and equation (13) for Δz at each time step. Thus at each time step the moments, change in velocity, change in hinge position and the new angle θ are calculated. As the plate is deforming as a membrane in tension and as there is a reduced section at the plug/plate interface, the expected failure is a tensile fracture at that point. A suitable failure criterion is required to calculate the amount of membrane stretching before fracture.

Consider the simplification that in stretching as a membrane in tension the plate behaves as a linearly tapered tensile sample and has linear strain hardening of the form

$$\sigma = \alpha + \beta\epsilon \tag{14}$$

where σ is the flow stress and

ϵ is engineering strain,

α and β are constants.

The situation is depicted in Fig. 4, and considering the plate as stretching radially from the plug diameter, the angle of taper is 2π. The strain at any position, under these conditions, is inversely proportional to radial

position, and the mean strain, ϵ_m, in the membrane can be related to the strain ϵ_o at the inside radius R_o and the maximum radius of yielding, R_1, by

$$\epsilon_m = \left[\frac{R_1 R_o}{(R_1 - R_o)^2} \ln \frac{R_1}{R_o} - \frac{R_1}{(R_1 - R_o)} + 1\right] \epsilon_o \qquad (15)$$

In the particular case of linear work hardening

$$\frac{R_1}{R_o} = 1 + \frac{\beta}{\alpha} \epsilon_o \qquad (16)$$

Thus the mean strain is given in terms of the strain at R_o by

$$\epsilon_m = \left[\frac{\alpha(\alpha + \beta \epsilon_o)}{\beta^2 \epsilon_o} \ln \left(\frac{\alpha + \beta\epsilon_o}{\alpha}\right) - \frac{\alpha}{\beta}\right] \qquad (17)$$

At fracture ϵ_o equals ϵ_f, the fracture strain in tension of the material. Thus equation (17) gives a value for the mean membrane strain in the dished material at fracture in terms of the material characteristics α, β and ϵ_f. ϵ_f can be obtained from a simple tension test and α and β by fitting the material stress/strain characteristics to equation (14).

In carrying out the calculations of stage II, the change in angle of dishing $\Delta\theta$ in each step is converted into an increment of mean membrane strain $\Delta\epsilon_m$. At each step the cumulative mean membrane strain within the dished region, which extends to the hinge at position z, is summed till equation (17) is satisfied with ϵ_o equal to ϵ_f for the material. At this point the plate is considered perforated due to fracture at the periphery of the plug. This approach to failure is very simplified in many aspects, including the use of engineering strains, the assumption of a uniaxial stress state in a tapered tensile geometry for the membrane stretching of the plate, the incrementing of strains with changes in dishing angle, and the simplified approach to the material properties. The method has however provided a consistent picture when applied to a number of cases which have been examined and is used at this stage for want of a more rigorous incremental procedure.

As the model is for the consideration of impacts below conventional ordnance velocities consideration must be given to the possible effects of clamping of the target plate if this is close enough to the impact site to influence the plate deformation. This is easily done computationally by including an option for the maximum value of the hinge position z as the position of the clamp.

The program listing of the structural model called DASH is given in the Appendix with a typical listing of input data. A variety of output

parameters are provided for, and a typical output listing is given for the input data provided.

4. DISCUSSION AND COMPARISON OF MODEL RESULTS

The simple analytical models presented restrict the deformation considerations to one simplified mode in each case. The structural model on the other hand allows for bending and stretching of the plate as well as shearing of a plug. The mechanism of plug separation for thin plates described in the model can be by a tensile failure or a shear fracture depending on the material and impact velocity, and this is in accord with observations of plug separation in thin plates. For example, Fig. 5 taken from Levy and Goldsmith [21] is one of many examples clearly illustrating the tensile separation of a plug. Shear failures by sliding off the plug are described in the model for thick targets and higher velocities of impact and this occurs directly from stage I. Thus the structural model conforms qualitatively with experience.

Shadbolt et al. [16] present a comparison of several models with experimental data for perforation velocity as a function of thickness for mild steel, aluminium alloy and stainless steel targets. The same data are compared with the analytical solutions for ductile hole formation failure, equation (1), dishing failure, equation (2), and plugging failure, equation (3), as well as the structural model in Fig. 6. It is noted that in each case the simple plugging solution greatly underestimates the critical velocity, whereas the experimental data generally lie between the ductile hole formation and dishing solutions. The structural model gives similar results to the dishing solution. Examination of the energy absorbed by different deformation modes, membrane, shearing and bending work, in the structural model gave very similar results to the approximate experimental estimates of Corran et al. [15] for the mild steel shots. Whilst the use of the structural model is a better approach these comparisons indicate the degree to which the simpler solutions can be used as useful approximations.

Scale up to larger size missiles can be assessed to some degree using the results of Neilson [23] produced at the Atomic Energy Establishment, Winfrith, UK, for impacts on mild steel plates from 1 to 25 mm thick. Missile diameters up to 85 mm and masses to 20 kg were used. Table I compares computations using the structural model with the experimental data. Given the need to estimate material properties the agreement is good. For the tests A and B using the lower strength steel the only difference was the span width of the target which influenced the model solution in the correct manner. For all other examples the span was sufficient that it did not influence the calculated critical perforation velocity.

As the objective is to give a more general solution which can be applied to estimate behavior with limited knowledge of material data and only a broad appreciation of the likely impact conditions the structural model was also tested for the impact of spheres on hollow steel tubes. Photographs of

typical failures observed by Xiaoqing and Stronge [22] showed that the basic deformation modes involve dishing and plugging, so that even though there is curvature in the target it is worth examining the structural model to see if it can be used to estimate ballistic limit velocities for various tube wall thicknesses and ball diameters. The comparison of experimental data with the calculated solutions in Fig. 7 again shows a correct order of magnitude estimate and correct trends with projectile diameter and tube thickness.

The diverse cases examined show the areas of applicability of the structural model and that it can be relied upon to give useful broad predictions of behaviour within what is acceptably possible from the theory of plasticity. The structural model and the simple analytical solutions are in a form which can easily be applied by practising engineers. A particularly valuable aspect is that rapid estimates of the influence on design variations of factors such as projectile diameter and mass and target thickness and material characteristics, can be obtained.

5. CONCLUSION

This report outlines two approaches to making estimates of the resistance of thin plates to perforation by low velocity impacts. One technique uses a set of analytical equations and the alternative method uses a structural model which requires a computer solution. The approaches are compared with published experimental data for projectile impacts to indicate the level of certainty expected from predictions. The essential purpose of the methods is to give guidance on the overall level of protection offered by a plate where the material properties are not accurately known, impact conditions are only broadly defined and experiments are not possible.

6. REFERENCES

1. Taylor, G.I. (1948). "The Formation and Enlargement of a Circular Hole in a Thin Plastic Sheet", Quart. J. Mech. Appl. Math. 1, 103-124.

2. Thomson, W.T. (1955). "An Approximate Theory of Armor Penetration", J. Appl. Phys. 26, 80-82.

3. Woodward, R.L. (1978). "The Penetration of Metal Targets by Conical Projectiles", Int. J. Mech. Sci. 20, 349-359.

4. Woodward, R.L. (1979). "Penetration Behaviour of a High Strength Aluminium Alloy", Metals Technology, 6, 106-110.

5. Woodward, R.L. (1978). "The Penetration of Metal Targets which Fail by Adiabatic Shear", Int. J. Mech. Sci. 20, 599-607.

6. Awerbuch, J. and Bodner, S.R. (1974). "Analysis of the Mechanics of Perforation of Projectiles in Metallic Plates", Int. J. Solids Structures, 10, 671-684.

7. Woodward, R.L. and de Morton, M.E. (1976). "Penetration of Targets by Flat Ended Projectiles", Int. J. Mech. Sci. 18, 119-127.

8. Backman, M.E. and Goldsmith, W. (1978). "The Mechanics of Penetration of Projectiles into Targets", Int. J. Engng. Sci. 16, 1-99.

9. Woodward, R.L. (1984). "The Interrelation of Failure Modes Observed in the Penetration of Metallic Targets", Int. J. Impact Engng. 2, 121-129.

10. Jonas, G.H. and Zukas, J.A. (1978). "Mechanics of Penetration: Analysis and Experiment", Int. J. Engng. Sci., 16, 879-904.

11. Zukas, J.A. (1980). "Impact Dynamics" in "Emerging Technologies in Aerospace Structures, Design, Structural Dynamics and Materials", Ed. J.R. Vinson, ASME August (1980), San Francisco, Ca., 161-198.

12. Wilkins, M.L. (1978). "Mechanics of Penetration and Perforation", Int. J. Engng. Sci. 16, 793-807.

13. Zukas, J.A., Nicholas, T., Swift, H.F., Greszczuk, L.B. and Curran, D.R. (1982). "Impact Dynamics", John Wiley & Sons, New York.

14. Bai, Y.L. and Johnson, W. (1982). "Plugging: Physical Understanding and Energy Absorption", Metals Technology, 9, 182-190.

15. Corran, R.S.J., Shadbolt, P.J. and Ruiz, C. (1983). "Impact Loading of Plates - an Experimental Investigation", Int. J. Impact Engng. 1, 3-22.

16. Shadbolt, P.J., Corran, R.S.J. and Ruiz, C. (1983). "A Comparison of Plate Perforation Models in the Sub-Ordnance Impact Velocity Range", Int. J. Impact Engng. 1, 23-49.

17. Liss, J., Goldsmith, W. and Kelly, J.M. (1983). "A Phenomenological Penetration Model of Plates", 1, 321-341.

18. Yuan Wenxue, Zhou Lanting, Ma Xiaoqing and Stronge, W.J. (1983). "Plate Perforation by Deformable Projectiles - A Plastic Wave Theory", Int. J. Impact Engng. 1, 393-412.

19. Liss, J. and Goldsmith, W. (1984). "Plate Perforation Phenomena Due to Normal Impact by Blunt Cylinders", Int. J. Impact Engng. 2, 37-64.

20. Levy, N. and Goldsmith, W. (1984). "Normal Impact and Perforation of Thin Plates by Hemispherically-Tipped Projectiles - I. Analytical Considerations", Int. J. Impact Engng. 2, 209-229.

21. Levy, N. and Goldsmith, W. (1984). "Normal Impact and Perforation of Thin Plates by Hemispherically-Tipped Projectiles - II. Experimental Results", 2, 299-324.

22. Ma Xiaoqing and Stronge, W.J. (1985). "Spherical Missile Impact and Perforation of Filled Steel Tubes", Int. J. Impact Engng. 3, 1-16.

23. Neilson, A.J. (1985). "Empirical Equations for the Perforation of Mild Steel Plates", Int. J. Impact Engng. 3, 137-142.

24. Duffey, T.A., Cheresh, M.C. and Sutherland, S.H. (1984). "Experimental Verification of Scaling Laws for Punch-Impact-Loaded Structures", Int. J. Impact Engng. 2, 103-117.

25. Symonds, P.S. (1968). "Plastic Shear Deformations in Dynamic Load Problems" in Engineering Plasticity, Ed. J. Heyman, and F.A. Leckie, Cambridge Univ. Press, London, 647-664.

26. Woodward, R.L. "A Structural Model for Thin Plate Perforation", Submitted to Int. J. Impact Engng.

27. Grzebieta, R.H. and Murray, N.W. (1985). "The Static Behaviour of Struts with Initial Kinks at their Centre Point", Int. J. of Impact Engng. 3, 155-165.

28. Murray, N.W. (1983). "The Static Approach to Plastic Collapse and Energy Dissipation in Some Thin-Walled Steel Structures" in Structural Crashworthiness, Ed. N. Jones and T. Wierzbicki, Butterworths, London, 44-65.

TABLE I

Comparison of Neilson [23] Data with Structural Model Calculations

DESIGNATION	SPAN WIDTH (mm)	TARGET THICKNESS (mm)	PROJECTILE DIAMETER (mm)	PROJECTILE MASS (kg)	UTS* (MPa)	V_c EXPERIMENT (ms^{-1})	V_c CALCULATION (ms^{-1})
A	220	1.0	32	4.3	320	12.5	17.5
B	127	1.0	32	4.3	320	9.5	12.5
C	588	15	63	19.8	470	80	75
D	588	25	63	19.8	470	102	101
E	1500	6	85	9.72	473	79	65
F	1500	12	85	9.72	473	99	91
G	1500	6	43	1.22	473	98	91
H	280	1.0	40	1.0	420	43	42
I	280	3.0	40	1.0	420	83	67

* Parameters used for structural model calculations (equation 14)

A and B Yield strength (Y) = α = 220 MPa, β = 360 MPa, ϵ_f = .37

C to I Yield strength (Y) = α = 340 MPa, β = 260 MPa, ϵ_f = .37

APPENDIX

The computer program for solution of the structural model is called DASH. The input file is called DASI.DAT and there are three output files DASF.DAT, DASA.DAT and DASO.DAT. The units for input data are indicated in Table A1 and all calculations and output are in SI units. There are a limited number of comment statements in the program to identify the major steps and the output parameters. For problems where the width of span is unimportant, 99999. will assume the plate is of infinite span. In other cases the maximum hinge position is limited by the input width of span. Table A2 gives a typical output listing for the data of Table A1.

TABLE A1

Typical Input - DASI.DAT (Mild steel target)

Parameter	Value	Units
Projectile diameter	12.7	mm
Target thickness	3.0	mm
Target density	7.8	g cm^{-3}
Target yield strength	220.	MPa
Projectile mass	.0346	kg
Impact velocity	100.	ms^{-1}
α (equation 14)	220.	MPa
β (equation 14)	360.	MPa
Fracture strain (ϵ_f)	.37	dimensionless
Span Width	99999.	mm

TABLE A2

Typical Output - DASO.DAT*

T	H	Z	V	X
0.000118	0.00202	0.0184	35.6	0.0067

PKE	WS	WB	WT	RKE	TE
23.9	12.5	62.6	30.3	7.1	136.4

* see program listing for identification of symbols

LISTING OF PROGRAM DASH

```
C     DASH.FOR
C     PROGRAM FOR PENETRATION OF THIN TARGETS
C     WRITTEN BY RAYMOND L WOODWARD,DEPT OF DEFENCE,
C               MATERIALS RESEARCH LABORATORIES,
C               MARIBYRNONG 1986
      OPEN(UNIT=1,FILE='DASI.DAT',STATUS='OLD')
      OPEN(UNIT=2,FILE='DASF.DAT',STATUS='NEW')
      OPEN(UNIT=3,FILE='DASA.DAT',STATUS='NEW')
      OPEN(UNIT=4,FILE='DASO.DAT',STATUS='NEW')
   21 FORMAT(F10.2/F10.2/F6.3/F7.1/F10.3/F7.1/F7.1/F7.1/F5.3/F8.1)
   23 FORMAT(F10.8,4X,F10.1,4X,F10.1,4X,F10.1,4X,F10.1,4X,F8.5,4X,F12.3
     1,4X,F10.5,4X,F10.5)
   22 FORMAT(F10.8,4X,F10.5,4X,F10.5,4X,F10.5,4X,F10.1,4X,F10.1,4X,F6.1
     1,4X,F6.1)
   24 FORMAT(3X,F10.6/3X,F10.6/3X,F8.1/3X,F12.0/F10.5/3X,F6.1,
     1/3X,F12.0/3X,F12.0/3X,F6.3/3X,F8.1/3X,F12.1)
   25 FORMAT(2X,F10.6,2X,F8.5,2X,F8.4,2X,F6.1,2X,2X,F8.4,F10.1,2X,F10.1
     1,2X,F10.1,2X,F10.1,2X,F10.1,2X,F10.1,2X,F10.1,2X,F10.1)
   28 FORMAT(F10.8,4X,F10.5,4X,F10.5,4X,F6.2,4X,F10.1,4X,F10.1,4X,F10.1
     1,4X,F10.1,4X,F10.1,4X,F6.1)
   26 FORMAT(T4,'PROJECTILE THROUGH')
   27 FORMAT(T4,'PROJECTILE STOPPED')
   29 FORMAT(T4,'TIME EXCEEDED')
   64 FORMAT(6X,'T'10X,'H'10X,'Z'10X,'V'10X,'X'9X,'PKE'9X,'WS'9X,'
     1WB'9X'WT'9X,'RKE'9X,'TE')
   65 FORMAT(6X,'T'12X,'Z'12X,'X'14X,'XP'12X,'PKE'10X,'TE'10X,'V'
     110X,'VP')
   66 FORMAT(6X,'T'14X,'PKE'12X,'WS'11X,'WB'12X,'RKE'9X,'H'
     114X,'BMI'11X,'Z1',11X,'Z2')
   67 FORMAT(6X,'T'12X,'Z'12X,'X'12X,'THO'12X,'WB'12X,'RKE'12X,'WT'
     111X,'PKE'12X,'TE')
      READ(1,21)DO,HO,RHO,SO,ASS,VEL,ALPA,BETA,EF,SPAN
C
C     DO  PROJ DIAM MM
C     HO  TARGET THICKNESS MM
C     RHO  TARGET DENSITY GM/CC
C     SO  TARGET YIELD STRENGTH MPA
C     ASS  PROJ MASS KG
C     VEL  PROJ VEL M/S
C     ALPA  STRAIN HARDENING RELATION TARGET
C     BETA  YS=ALPA+BETA*STRAIN  (MPA)
C     EF  FRACTURE STRAIN IN TENSION TEST
C     SPAN TOTAL WIDTH OF TEST PIECE MM IF UNIMP. USE 99999.
C
      HO=HO/1000
      RO=DO/2000
      RHO=RHO*1000
      SO=SO*1000000.
      ALPA=ALPA*1000000.
      BETA=BETA*1000000.
      ZMAX=(SPAN-DO)/2000
      EMP=EF*((ALPA*(ALPA+BETA*EF)/((BETA*EF)**2))*ALOG(1+BETA*EF/
     1ALPA)-ALPA/(BETA*EF))
      SKE=ASS*(VEL**2)/2
      T=0
```

```
      H=HO
      EMO=6.28318*RHO*HO
C     QI IS SHEAR FORCE INTEGRAL
      QI=0
C     BMI IS BENDING MOMENT INTEGRAL
      BMI=0
      WB=0
      WS=0
      WT=0
      F1=ASS*VEL
      RO2=RO**2
      RO3=RO**3
      F2=ASS+EMO*(RO**2)/2
      X=0
      XP=0
      Z1=0
      Z2=0
C     TIME STEP FOR FIRST STAGE
      DT=.008019*ASS*VEL*RHO*RO/((ASS+4.044*RHO*HO*(RO**2))*SO)
C
C     WRITES OUT INPUT,SKE=INITIAL KE
      WRITE(4,24)DO,HO,RHO,SO,ASS,VEL,ALPA,BETA,EF,SPAN,SKE
      WRITE(4,64)
      WRITE(2,65)
      WRITE(3,66)
C
C     INITIAL PHASE OF BENDING AND SHEARING TILL VEL BENDING PLATE
C     EQUALS PLUG/PROJ VEL
C
      DO 72 I=1,500
      QP=1.814*H*SO*RO
      QI=QI+2*QP*DT
      VP=(F1-QI)/F2
      IF(VP.LE.V)GO TO 73
      A=-3*QI
      B=RO*QI-2*BMI
      C=6*BMI*RO
      Z1=(-B+SQRT((B**2)-4*A*C))/(2*A)
      Z2=(-B-SQRT((B**2)-4*A*C))/(2*A)
      Z=Z2
      V=2*QI/(EMO*Z*(RO+Z/3))
      X=X+V*DT
      XP=XP+VP*DT
      H=HO-(XP-X)
      PKE=F2*(VP**2)/2
      WS=WS+2*QP*(VP-V)*DT
      IF(Z.GT.0)GO TO 32
      WB=WB+0
      GO TO 33
   32 WB=WB+1.5708*SO*V*DT*(RO*(H**2)+(RO+Z)*(HO**2))/Z
   33 RKE=1.0471*HO*RHO*Z*(RO+Z/4)*(V**2)
      TE=PKE+WS+WB+RKE
      T=T+DT
      BMI=BMI+(RO*(H**2)+(RO+Z)*(HO**2))*.7853*SO*DT
C
C     OUTPUT DASF.DAT
C     T-TIME,Z-HINGE POSITION,X-DISPL. PLATE,XP-DISPL. PLUG,
C     PKE-PROJ. KE,TE-TOTAL ENERGY,V-VEL PLATE,VP-VEL PLUG.
      WRITE(2,22)T,Z,X,XP,PKE,TE,V,VP
C
```

```
C     OUTPUT DASA.DAT
C     T-TIME,PKE-PROJ. KE,WS-WORK SHEAR,WB-WORK BENDING,RKE-ROTATIONAL KE,
C     H-PLUG/PLATE CONTACT LENGTH,BMI-BEND MMT INTEGRAL,
C     Z1-INVALID QUADRATIC ROOT,Z2-VALID ROOT HINGE POSITION.
      WRITE(3,23)T,PKE,WS,WB,RKE,H,BMI,Z1,Z2
      IF(H.LE.0)GO TO 75
      IF(VP.LT..1)GO TO 76
   72 CONTINUE
C
C     SECOND STAGE OF BENDING AND STRETCHING TILL FRACTURE
C     CONDITION EXCEEDED
C
   73 V=VP
      THR=ATAN2(X,Z)
      ENTR=Z/COS(THR)
      FT=6.2832*RO*H*SO
      THE=THR
      THP=THR
      ZP=Z
      EREF=(1/COS(THR))-1
C
C     TIME STEP SET FOR SECOND PHASE
C
      DT=HO/(25*VEL)
      EM=0
      WRITE(2,67)
      DO52 N=1,5000
      SMP=1.5708*SO*(RO+Z)*(HO**2)
      SMPP=SMP*(1-(RO*H/((RO+Z)*HO))**2)
      DV=(-SMPP-FT*Z*SIN(THE))*DT*2/((F2+EMO*Z*(RO+Z/4)/3)*Z*COS(THE))
      DZ=(-F2*DV-EMO*DV*Z*(RO+Z/3)*DV/2)/(6.283*(RO+.6667*Z)*HO*RHO*V)
      V=V+DV
      X=X+V*DT
      THE=ATAN2(X,Z)
      DEM=1/COS(THE)-1/COS(THP)
      WB=WB+(SMPP+FT*Z*SIN(THE))*(THE-THP)
      Z=Z+DZ
      IF(SPAN.GT.99998.)GO TO 109
      IF(Z.LE.ZMAX)GO TO 109
      Z=ZMAX
  109 PKE=F2*(V**2)/2
      RKE=1.0471*HO*RHO*Z*(RO+Z/4)*(V**2)/(COS(THE)**2)
      WT=WT+FT*COS(THE)*(ZP/COS(THE)-ZP/COS(THP))
      ZP=Z
      THP=ATAN2(X,Z)
      TE=PKE+WS+WB+RKE+WT
      T=T+DT
      EM=EM+DEM
      THO=THE*57.296
      IF(EMF.LE.(EM-EREF))GO TO 75
      IF(V.LT..1)GO TO 76
      DO 83 I=1,200
      INC=I*25
      IF(N-INC)52,53,83
   83 CONTINUE
C
C     OUTPUT DASF.DAT
C
C     T-TIME,Z-HINGE POS,X-DISPL. PLATE,THO-BEND ANGLE PLATE DEGREES
C     WB-WORK BENDING,RKE-ROTAT. KE,WT-MEMBRANE WORK,
```

```
C     PKE-PROJ. KE,TE-TOTAL ENERGY.
   53 WRITE(2,28)T,Z,X,THO,WB,RKE,WT,PKE,TE
   52 CONTINUE
      WRITE(4,29)
      GO TO 77
   75 WRITE(4,26)
      GO TO 77
   76 WRITE(4,27)
C
C     OUTPUT DASO.DAT
C     MAJOR OUTPUT PARAMETERS,T-TIME, H-PLUG/TARGET CONTACT LENGTH,
C           Z-FINAL HINGE POSITION, V-PLUG/PROJ VEL, X-DISHING AMT,
C           PKE-PROJ KE, WS-WORK SHEAR, WB-WORK BENDING, WT-TENSION WORK,
C           RKE-ROTARY KE OF PLATE, TE-TOTAL ENERGY
C
   77 WRITE(4,25)T,H,Z,V,X,PKE,WS,WB,WT,RKE,TE
      STOP
      END
```

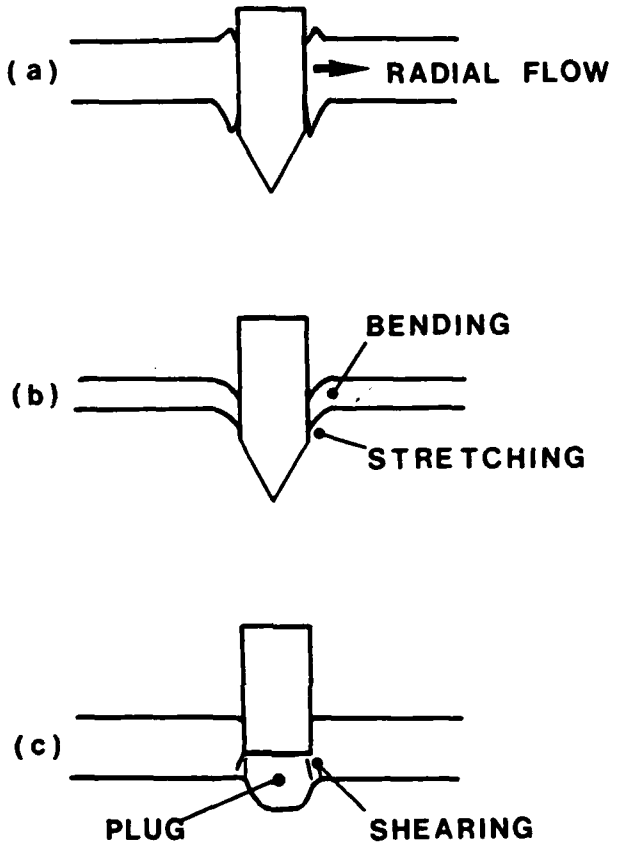

FIGURE 1 Mechanisms of failure of ductile metal targets. (a) Ductile hole formation failure, (b) dishing failure and (c) plugging failure.

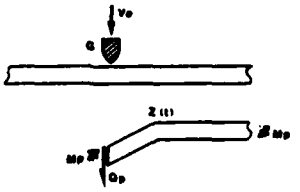

FIGURE 2 Impact of a mass G with velocity V_0 on an infinite beam. Shearing and bending occurs at the impact site and bending at a hinge, distance z from impact.

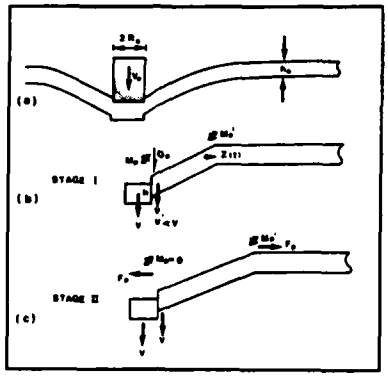

FIGURE 3 Impact of a projectile on an infinite plate. (a) Schematic section, (b) Stage I in which shearing of the plug occurs, and (c) Stage II in which membrane stretching of the plate occurs.

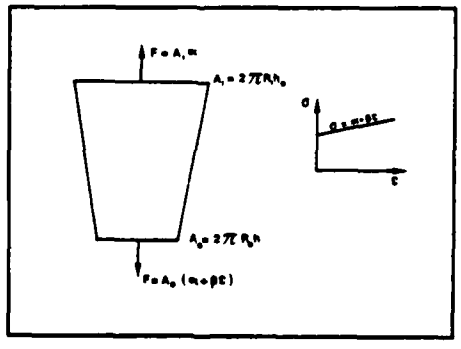

FIGURE 4 Treatment of the plate in Stage II as a tapered tensile sample with material properties characterised as rigid/linear work hardening. The arrows indicate the application of the tensile force and, as the radial stretching of a plate is being considered, the angle of taper is 2ψ.

FIGURE 5 Perforated plate showing the dishing and plug separation associated with perforation by a blunt projectile. The failure mechanism is a tensile fracture. From Levy and Goldsmith [21].

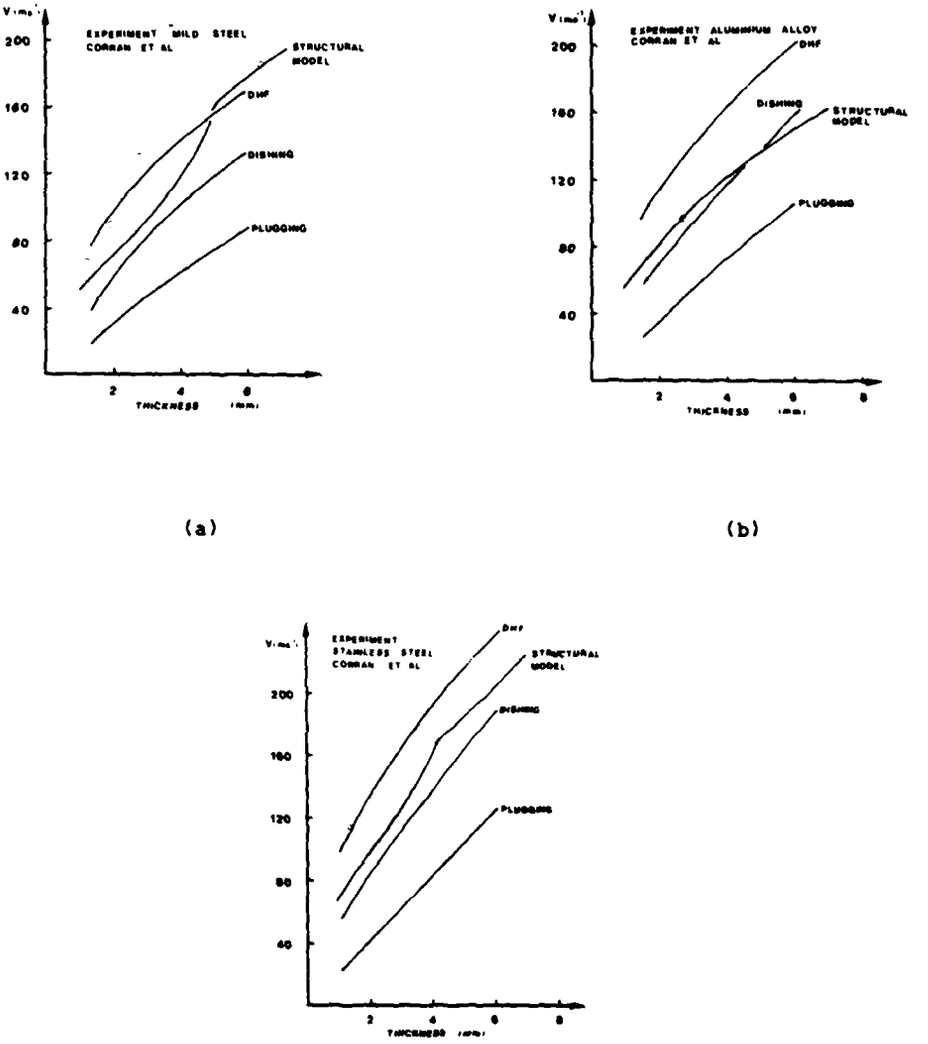

(a) (b)

(c)

FIGURE 6 Comparison of Solutions using the models for ductile hole formation (DHF), equation (1), dishing, equation (2), plugging, equation (3), and the structural model with the experimental data of Corran et al. [15,16]. (a) Mild steel targets, (b) aluminium alloy targets and (c) stainless steel targets.

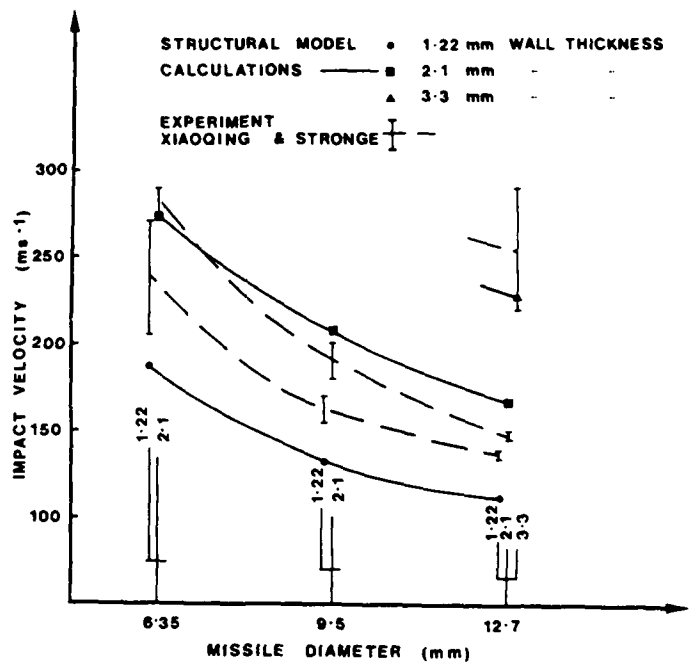

FIGURE 7 Comparison of empirical data from Xiaoqing and Stronge [22] for tubes of different wall thickness and for different projectile diameters with predictions using the structural model. Results are offset at each missile diameter to distinguish the different tube size results more clearly.

END

DATE
FILMED

6-87